JOURNAL OF SOLID STATE CHEMISTRY 75, 188–196 (1988)

Novel Defect Pyrochlores $A\mathrm{Bi}_2B_5\mathrm{O}_{16}$ (A = Cs, Rb; B = Ta, Nb)

M. K. EHLERT AND J. E. GREEDAN

Institute for Materials Research and Department of Chemistry, McMaster University, Hamilton, Canada L8S 4M1

AND M. A. SUBRAMANIAN

Central Research and Development Department, E. I. DuPont de Nemours and Co., Experimental Station, Wilmington, Delaware 19898*

Received August 17, 1987; in revised form February 1, 1988

The crystal structures of three oxides with compositions $CsBi_2Nb_5O_{16}$, $CsBi_2Ta_5O_{16}$, and $RbBi_2Ta_5O_{16}$ have been determined from powder neutron diffraction data. A common structure of the defect pyrochlore type has been found. Atomic positions in space group $Fd3m$ are 3.2 O and 3.2 Cs(Rb) in 8b, 6.4 Bi in 16d, 16 Ta(Nb) in 16c, and 48 O in 48f. There is some evidence that the Rb atoms actually occupy 32e sites. On electrostatic grounds it is highly unlikely that the Cs(Rb) and O atoms are randomly distributed in 8b. Evidence for short-range order is apparent in the X-ray powder diffraction data. Cell constants are 10.528(1) Å (Cs, Nb), 10.504(1) Å (Cs, Ta), and 10.510(2) Å (Rb, Ta), respectively, with 48f x parameters 0.3139(2) (Cs, Nb), 0.3152(2) (Cs, Ta), and 0.3153(2) (Rb, Ta). Isotropic temperature factors for the 8b and 16d site atoms ranged from 3 to 6 $(Å)^2$. These large values suggest anharmonic behavior or high mobility for some of the ions. Evidence for this is found in the presence of significant dielectric loss effects in all of the compounds studied.

Introduction

Materials with the pyrochlore structure are numerous and exhibit a rich crystal chemical variety. Oxide pyrochlores have recently been reviewed. (*1*). The ideal pyrochlore structure of composition $A_2B_2X_6X'$ can be described in space group $Fd3m$, $z = 8$, with A in 16d, B in 16c, X in 48f, and X' in 8b.

A number of defect or nonstoichiometric pyrochlores also exist. In such materials the 16c and 48f sites are always fully occupied, consistent with calculations which show that the B_2X_6 network formed by these sites accounts for 80% of the electrostatic binding energy (*2*). Thus, defect pyrochlores are characterized by vacancies on either the 16d, 8b, or related sites leading to compositions such as $A_2B_2X_6$ or AB_2X_6. A number of examples of the latter type are known where X is O or F. The A species is normally a large monovalent cation such as Cs, Rb, K, or Tl and B is a pentavalent transition metal such as Ta or Nb or a BB' combination of appropriate valences (*3–14*). Examples are $CsNiFeF_6$, $CsTa_2O_5F$, or $TlNb_2O_5F$. In general, the large monovalent species, such as Cs, occupy the vacant 8b sites while smaller cations such as Rb and Tl have been found in 32e sites (*15*).

In this work, the preparation and struc-

---

* Contribution No. 4410.

0022-4596/88 $3.00

tural characterization of a series of novel defect pyrochlores of compositions $CsBi_2Ta_5O_{16}$, $CsBi_2Nb_5O_{16}$, and $RbBi_2Ta_5O_{16}$ are described. Letting A = Cs or Rb and B = Nb or Ta, the contents of one pyrochlore-type cell can be written as $A_{3.2}Bi_{6.4}B_{16}O_{48}O'_{3.2}$. Thus, these materials would appear to present the possibility for high-defect concentrations on both the 16d and 8b or 32e sites. In order to confirm a defect pyrochlore model for these compounds and to determine the site occupancies of the various species, neutron powder diffraction studies were carried out. The influence of such defect concentrations on the dielectric loss of these materials was also investigated.

Experimental

The compounds were prepared by firing the oxides of the component elements at 1050°C in air with regrinding and refiring.

X-ray powder diffraction data were obtained using a Nicolet I2 automated diffractometer.

Density measurements were obtained by pycknometry using nitrobenzene as the immersion liquid at 25°C.

Neutron powder diffraction data were obtained at the McMaster Nuclear Reactor using 1.3925-Å neutrons and a position-sensitive detector which has been described previously (*16*). Data refinement was done by the Rietveld method[1] (*17*). Gaussian line shapes were assumed. In addition to positional, thermal, and unit cell parameters, the scale, a zero point correction, and 3 half-width and 10 background (2 per frame) parameters were refined.

Dielectric Properties

The dielectric constant and loss factors were measured at frequencies ranging from 10^3 to 10^7 Hz under weak *ac* fields using Hewlett–Packard (4274A and 4275A) automating LCR bridges. The samples were in the form of sintered pellets with sputtered gold as electrodes and in some cases the measurements were done from room temperature to 250°C. Measurement details were described elsewhere (*18*).

Results and Discussion

Crystal Structure

The X-ray powder diffraction patterns for all three materials could be indexed on a cubic cell with systematic absences consistent with space group $Fd3m$. These results are shown in Table I. In addition to the Bragg reflections, broad diffuse-scattering features were evident in the powder patterns of all three materials. These will be discussed later.

As an initial model for refinement of the neutron diffraction data, the Ta(Nb) atoms, $\frac{15}{16}$ of the O atoms, and the Bi atoms were assigned to sites 16c, 48f, and 16d, respectively, in $Fd3m$. This leaves the 8b site to accommodate both the Cs(Rb) atom and the remaining $\frac{1}{16}$ of the O atoms. The overall composition of one pyrochlore unit cell is then: $Bi_{6.4}Ta(Nb)_{16}O_{48}O'_{3.2}Cs(Rb)_{3.2}$. Refinement of all three data sets proceeded smoothly to the values listed in Table II. Figure 1 shows a typical data set illustrating the quality of the fit. Selected bond lengths and angles are given in Table III.

To our knowledge, these are unique pyrochlores in that defects exist on both the 16d and 8b sites and that, apparently, both oxide ions and monovalent cations are found in the same, 8b, site. Observed densities agreed well with those calculated assuming the proposed model. For $CsBi_2Nb_5O_{16}$, $CsBi_2Ta_5O_{16}$, and $RbBi_2Ta_5O_{16}$ the observed and calculated values are, respectively, 5.68(0.11) and 5.79, 7.71(0.15) and 7.85, and 7.52(0.15) and 7.61 g cm^{-3}.

---

[1] The version of the Rietveld program used here was modified by A. W. Hewat and E. Prince with further modifications added locally by M. Eitel.

TABLE I

X-RAY POWDER DATA FOR $Cs(Rb)Bi_2Ta(Nb)_5O_{16}$

	$CsBi_2Ta_5O_{16}$ $a_0 = 10.5030(6)$		$CsBi_2Nb_5O_{16}$ $a_0 = 10.5295(5)$		$RbBi_2Ta_5O_{16}$ $a_0 = 10.5121(4)$	
hkl	d (Å)	I_{Rel}	d (Å)	I_{Rel}	d (Å)	I_{Rel}
111	6.0564	11	6.062	3	6.0578	14
220	3.7115	1	3.7187	4		<1
311	3.1642	29	3.1711	17	3.1663	23
222	3.0298	100	3.0363	100	3.0318	100
400	2.6242	27	2.6300	19	2.6259	32
331	2.4079	1	2.4131	3	2.4100	1
422		<1		<1		<1
511, 333	2.0209	12	2.0260	<1	2.0224	9
440	1.8560	48	1.8610	53	1.8574	44
531	1.7748	51		<1	1.7767	6
442		<1		<1		
620	1.6607	1	1.6644	3	1.6606	1
533	1.6017	5	1.6048	3	1.6026	4
622	1.5870	52	1.5868	36	1.5844	38
444	1.5158	8	1.5194	7	1.5168	10
551, 711	1.4708	4	1.4740	2	1.4716	5
642		<1	1.3974	1		<1
731, 553	1.3676	13	1.3709	9	1.3687	10
800	1.3131	9	1.3162	9	1.3141	8
733	—	—	1.2841	1	1.2843	1
644	—	—	1.2706	1	1.2767	0
660, 822	—	—		<1	1.2387	1
751, 555	—	—	1.2158	2	1.2139	3
662	—	—	1.2079	16	1.2059	19
840	—	—	1.1774	9	1.1755	16
911, 753	—	—	1.1562	1	1.1539	4
842	—	—	1.1494	1		<1
664	—	—	1.1226	2	1.1208	1
931	—	—	1.1040	3	1.1021	3

The only unusual features found in Table II are the somewhat large thermal parameters for atoms in the 16d (Bi) and 8b (Cs, Rb, O′) sites. These observations led us to explore other possible sites.

First, the Bi atoms were placed in the 32e site but in all three cases the final parameters were indistinguishable from the 16d ($\frac{1}{2}$, $\frac{1}{2}$, $\frac{1}{2}$) site. Anisotropic thermal parameters were refined for the Bi atoms in 16d yielding the following results: $Bi_2Ta_5O_{15}O'Cs$, $B_{11} = B_{22} = B_{33} = 0.0117(3)$, $B_{13} = B_{23} = B_{12} = 0.0034(4)$, $R_{wp} = 0.0506$; $Bi_2Nb_5O_{15}O'$ Cs, $B_{11} = B_{22} = B_{33} = 0.0135(4)$, $B_{13} = B_{23} = B_{12} = -0.0038(5)$, $R_{wp} = 0.0535$; and $Bi_2Ta_5O_{15}O'Rb$, $B_{11} = B_{22} = B_{33} = -0.0108(4)$, $B_{13} = B_{23} = B_{12} = -0.0032(5)$, $R_{wp} = 0.0415$. These parameters, while large, are similar to those reported for Tl^+ in $TlNb_2O_5F$, a material with a high ionic conductivity (*10*).

In addition, Fourier difference techniques were used to determine the positions of the Cs and Rb atoms. For the two Cs compounds the only positive features on the difference map were at $\frac{3}{8}$, $\frac{3}{8}$, $\frac{3}{8}$, the 8b site. In the case of the Rb compound, how-

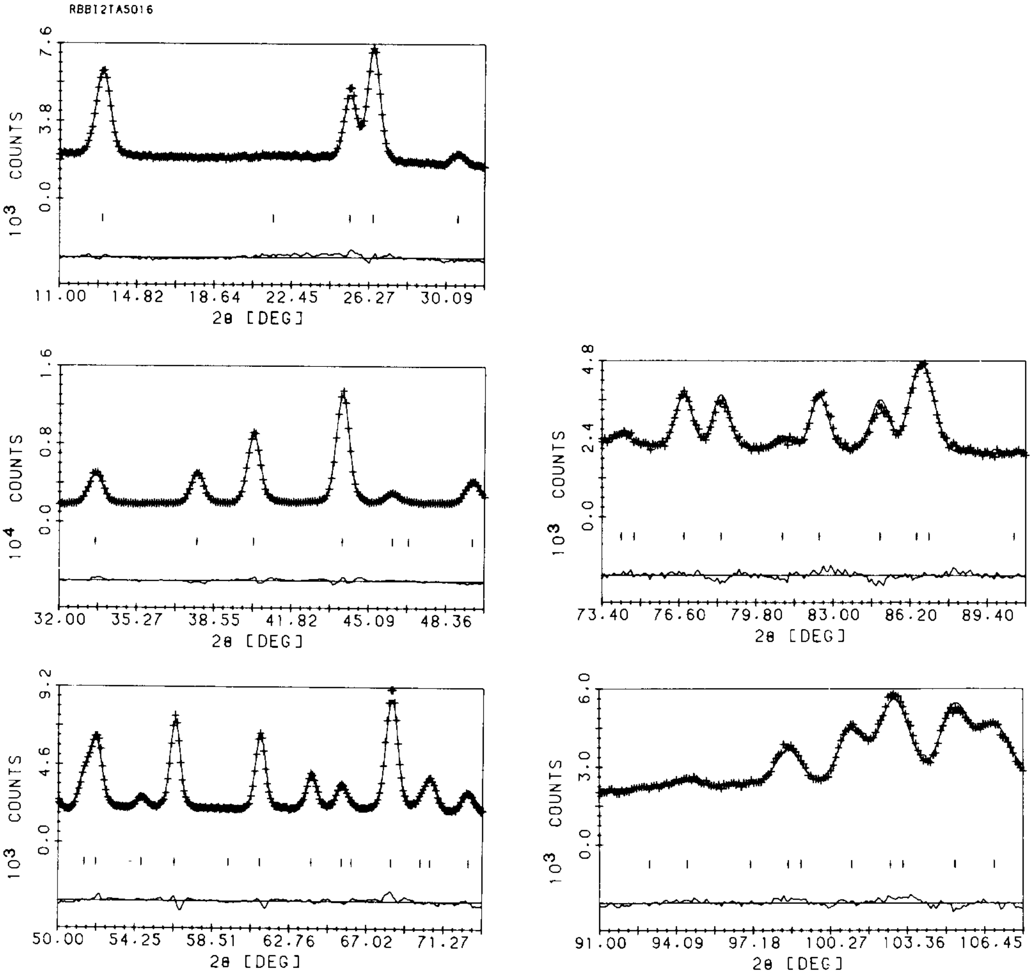

FIG. 1. Observed (+), calculated (−), and difference neutron powder diffraction profiles for $RbBi_2Ta_5O_{16}$. The positions of Bragg reflections are indicated.

ever, prominent features were evident at, approximately, 0.44, 0.44, 0.44 and related positions with a slight, negative difference at the 8b position. Although the evidence is consistent with Rb occupation of the 32e sites, refinement was strongly dependent on the starting position. In one case, beginning at $x = 0.425$ the refinement converged to $x = 0.404(1)$ with $R_{wp} = 0.0410$ and $B(\mathrm{Rb}) = 1.7(4)$ Å^2. Other starting positions resulted in refinement to nearby sites but with no improvement in R_{wp}, indicating that a rather shallow minimum is involved. In summary, for the two Cs materials, partial occupation of the 8b sites by both O and Cs ions seems confirmed, while reasonable evidence exists for delocalization of the Rb ion into a 32e site for that compound. This is consistent with the relative ionic sizes of Cs^+ and Rb^+ and with the findings of Fourquet *et al.* (*15*) for $CsNb_2O_5F$ and $RbNb_2O_5$ F; however, evidence for Rb occupation of the 32e positions is not so strong as in these cases.

TABLE II

POSITIONAL AND ISOTROPIC THERMAL PARAMETERS FOR THE DEFECT PYROCHLORES $Bi_2Ta(Nb)_5O_{15}O'Cs(Rb)$

$Bi_2Ta_5O_{15}O'Cs$			$Bi_2Nb_5O_{15}O'Cs$			$Bi_2Ta_5O_{15}O'Rb$		
Atom	Position	B (Å)^2	Atom	Position	B (Å)^2	Atom	Position	B (Å)^2
Bi	$\frac{1}{2}, \frac{1}{2}, \frac{1}{2}$	5.3(2)	Bi	$\frac{1}{2}, \frac{1}{2}, \frac{1}{2}$	6.1(2)	Bi	$\frac{1}{2}, \frac{1}{2}, \frac{1}{2}$	4.9(2)
Ta	0, 0, 0	0.52(4)	Nb	0, 0, 0	0.89(4)	Ta	0, 0, 0	0.45(4)
O	0.3153(1), $\frac{1}{8}, \frac{1}{8}$	0.87(3)	O	0.3139(1), $\frac{1}{8}, \frac{1}{8}$	1.11(3)	O	0.3156(1), $\frac{1}{8}, \frac{1}{8}$	0.74(3)
O′	$\frac{3}{8}, \frac{3}{8}, \frac{3}{8}$	3.28(9)	O′	$\frac{3}{8}, \frac{3}{8}, \frac{3}{8}$	3.5(1)	O′	$\frac{3}{8}, \frac{3}{8}, \frac{3}{8}$	5.4(1)
Cs	$\frac{3}{8}, \frac{3}{8}, \frac{3}{8}$	3.28(9)	Cs	$\frac{3}{8}, \frac{3}{8}, \frac{3}{8}$	3.5(1)	Rb	$\frac{3}{8}, \frac{3}{8}, \frac{3}{8}$	5.4(1)
a_0 =	10.505(1) Å		a_0 =	10.528(1) Å		a_0 =	10.508(1) Å	
R_N	0.0487		R_N	0.0566		R_N	0.0677	
R_p	0.0398		R_p	0.0427		R_p	0.0336	
R_{wp}	0.0523		R_{wp}	0.0552		R_{wp}	0.0427	
R_E	0.0204		R_E	0.0196		R_E	0.0163	
No. OBS	975		No. OBS	965		No. OBS	976	
No. *hkl*	63		No. *hkl*	67		No. *hkl*	64	
No. parameters	21		No. parameters	21		No. parameters	21	

$R_N = \Sigma|I_{obs} - I_{calc}|/\Sigma I_{obs}$

$R_p = (\Sigma|Y_{obs} - Y_{calc} \cdot \text{scale}|^2/\Sigma|Y_{obs}|^2)^{1/2}$

$R_{wp} = (\Sigma w|Y_{obs} - Y_{calc} \cdot \text{scale}|^2/\Sigma w(Y_{obs})^2)^{1/2}$; $w = 1/Y_{obs}$

$R_E = (\text{degrees of freedom}/\Sigma w(|Y_{obs}|)^2)^{1/2}$

Degrees of freedom = (number profile points) − (number of parameters)

Note. Cs and Rb atoms in 8b.

It should be mentioned here that an alternative understanding of the large observed thermal parameters can, in principle, be obtained by consideration of anharmonic thermal motions (*19–21*). This model has been applied with success to materials with similar features, for example, the solid electrolyte α-Ag_2HgI_4 (*22*), CaF_2 (*23*), and $MgAl_2O_4$ at elevated temperatures (*24*). In these cases, the atoms undergoing anharmonic motion have 43m or 3m site symmetry as do the 8b and 16d sites in pyrochlores, for example, F in CaF_2, Ag^+ and I^- in α-Ag_2HgI_4, Mg^{2+} in $MgAl_2O_4$, or Al^{3+} in $MgAl_2O_4$. This approach is presently under active consideration.

As pointed out earlier, these defect pyrochlores exhibit the unique feature that both the 16d and 8b sites are partially occupied by cationic species, yet, the 8b sites coordinate the 16d sites in pyrochlores. On electrostatic grounds, the most favorable distribution of ions among these sites is that Cs^+ or Rb^+ coordinate empty 16d sites while O^{2-} coordinates Bi^{3+}-filled 16 sites. In fact, one might expect the formation of clusters or domains based on the two possible coordination environments of the 16d sites.

Evidence for such clustering or short range order is seen in the prominent diffuse scattering feature of the x-ray powder diffraction patterns as illustrated in Fig. 2 for $CsBi_2Ta_5O_{16}$. Note the broad peak in the background near 26° (2θ). The FWHM of this peak is 8.0°(5) (2θ). Application of the Scherrer formula yields an estimate of 80 Å as the average cluster dimension.

It is significant to note that diffuse scattering effects are absent in the neutron powder diffraction data. Two factors probably contribute here. First, the background level is somewhat greater in the neutron experiment and, more importantly, the con-

TABLE III

BOND LENGTHS AND ANGLES FOR THE $ABi_2B_5O_{15}O'$ (A = Cs, Rb; B = Nb, Ta) COMPOUNDS (A IN 8b SITES)

	$CsBi_2Nb_5O_{15}O'$	$CsBi_2Ta_5O_{15}O'$	$RbBi_2Nb_5O_{15}O'$
A–O (Å)	3.7771(9)	3.767(1)	3.7676(7)[a]
Bi–O' (Å)	2.2793(4)	2.2744(4)	2.2751(3)
Bi–O (Å)	2.702(1)	2.685(1)	2.685(1)
B–O (Å)	1.9790(6)	1.9799(7)	1.9811(6)
O–Bi–O (°)	62.03(2)	62.14(2)	62.15(2)
O–Bi–O' (°)	57.72(2), 122.28(2)	57.81(2), 122.19(2)	57.82(2), 122.18(2)
O–B–O (°)	89.41(5), 90.59(5)	88.85(6), 91.15(6)	88.79(5), 91.21(5)
B–O–B (°)	140.23(8)	139.42(8)	139.34(8)

[a] For Rb in 32e, x = 0.404(1), Rb–O = 2.98(1) Å.

trast in scattering power between Bi (scattering length, $b = 0.853$), Cs ($b = 0.542$), Rb ($b = 0.708$), and O ($b = 0.581$) is much less in the neutron case than for X-rays.

Dielectric Properties

The results of the dielectric measurements on these same defect pyrochlores are given in Figs. 3 to 6. The measured dielectric constant of $CsBi_2Nb_5O_16$ is substantially higher than those of Ta-containing pyrochlores. For all the compounds, the dielectric constant data showed a frequency independent behavior at higher frequencies (>10^4 Hz); however, at low frequencies a sharp rise in the dielectric constant is

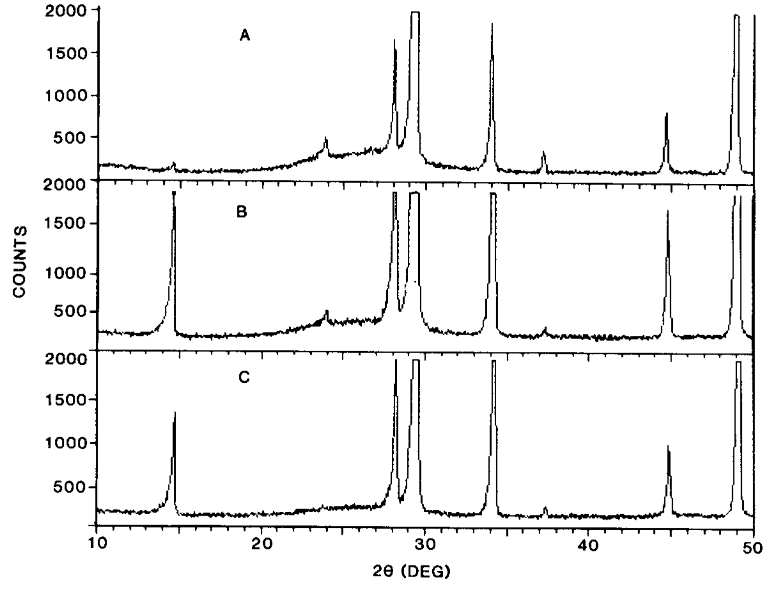

FIG. 2. X-ray powder diffraction data showing the presence of a diffuse feature near 26°. (A) $CsBi_2Nb_5O_{16}$, (B) $CsBi_2Ta_5O_{16}$, (C) $RbBi_2Ta_5O_{16}$.

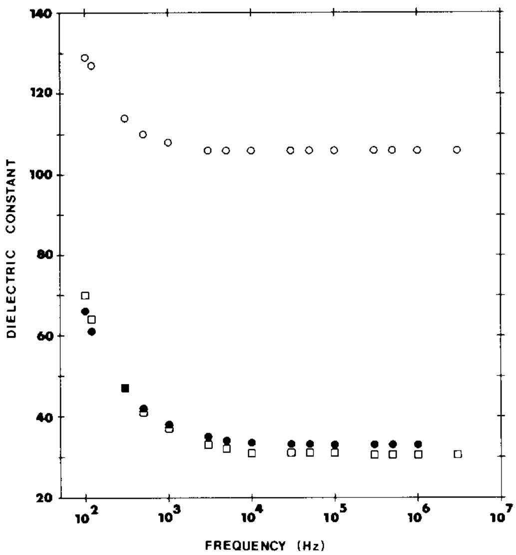

FIG. 3. Frequency dependence of the dielectric constant for the $ABi_2B_5O_{16}$ pyrochlores. ○ (Cs, Nb), □ (Cs, Ta), ● (Rb, Ta).

noted. Dielectric loss measurements of all the pyrochlores also showed a sharp increase at lower frequencies. As the measurement temperature was raised, dielectric loss showed a steep increase even at moderately higher frequencies (Fig. 4).

The observed dielectric behavior can be rationalized as follows. As shown earlier by neutron diffraction studies, all three pyrochlores have a large concentration of cation vacancies. The observed thermal parameters for the *A* and Bi cations are large, suggesting anharmonic behavior of these cations. Under an applied electric field, these cations can jump from an occupied site to a neighboring vacant site (vacancy mechanism) (*25*) giving rise to net ionic conductivity. In fact, many defect pyrochlores of the type $A_{1+x}B_2O_{6+y}$ were shown to have high ionic conductivity (*1*). The dielectric constant of a crystalline sample results from electronic, ionic, and dipolar orientation polarization. In addition to the above, in these pyrochlores, ion jump polarization is responsible for the increase in the dielectric constant at low frequencies ($<10^3$ Hz). As the temperature is raised, there is an increase in the contribution from cation mobility which increases exponentially with temperature. The result is a sharp rise in dielectric constant at low frequencies, corresponding to both ion jump orientation effects and space charge effects (concentration of charge carriers at the electrodes).

Dielectric loss in ionic solids results from three primary processes: (1) ion migration losses (dc conductivity and dipole relaxation), (2) ion vibration and deformation losses, and (3) electron polarization losses. Of these, the most important is the ion migration losses which tend to increase at low frequencies and as the temperature is raised. The observed sharp increase in the dielectric loss at lower frequencies for all three pyrochlores (Fig. 5) is largely due to the ion jump relaxation between two equivalent ion positions. If the applied frequency is larger than the jump frequency, the at-

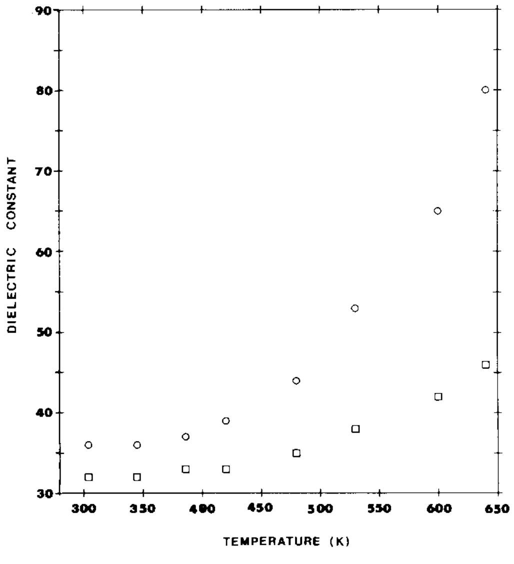

FIG. 4. Temperature dependence of the dielectric constant for $RbBi_2Ta_5O_{16}$ at 10^3 Hz (○) and 10^6 Hz (□).

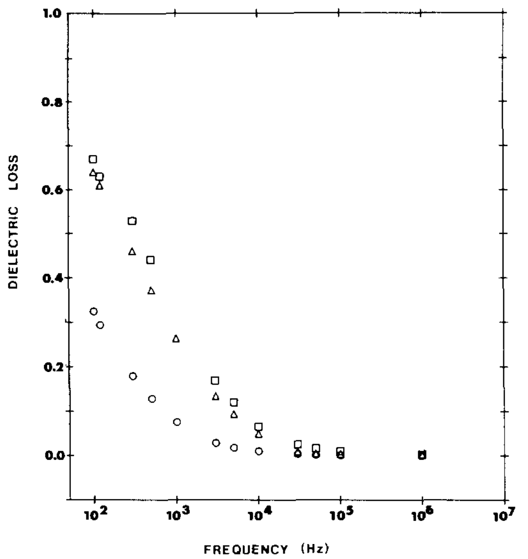

FIG. 5. Frequency dependence of the dielectric loss for $ABi_2B_5O_{16}$ pyrochlores: ○ (Cs, Nb), □ (Cs, Ta), △ (Rb, Ta).

oms do not have an opportunity to jump at all and the losses are small. For an ion jump the jump frequency depends on the energy barrier separating the two ion positions and the presence of energetically equivalent vacant sites. As the temperature is raised, the jump frequency of the ions increases exponentially which gives rise to higher dielectric losses at moderately high frequencies (10^3 to 10^6) (Fig. 6).

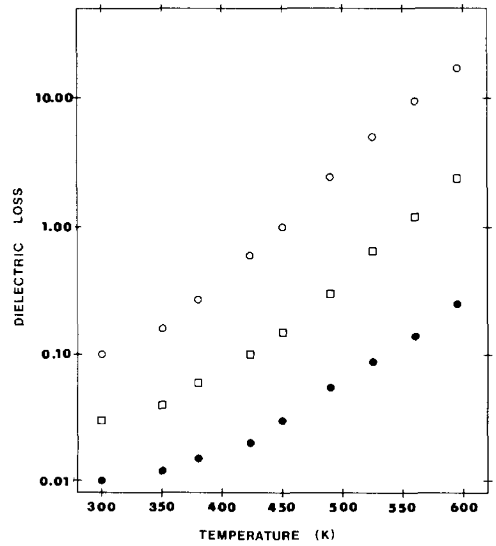

FIG. 6. Temperature dependence of the dielectric loss for $RbBi_2Ta_5O_{16}$ at 10^3 Hz (○), 10^4 Hz (□), and 10^6 Hz (●).

Although the above dielectric study is quite preliminary, the observed data seem to correlate well with the crystal structure of these pyrochlores determined by neutron diffraction. Further detailed dielectric relaxation studies on these interesting pyrochlores are in progress and will be published later.

Acknowledgments

We thank Messrs. J. N. Reimers and A. H. O'Reilly and Mrs. M. Crowe for assistance and useful discussions. Financial support to J.E.G. in the form of an operating grant and infrastructure support of the McMaster Nuclear Reactor was provided by the Natural Science and Engineering Research Council of Canada.

References

1. M. A. SUBRAMANIAN, G. AVRAVAMUDAN, AND G. SUBBA, RAO, *Prog. Solid State Chem.* **15,** 55 (1983).
2. J. PANNETIER, *J. Phys. Chem. Solids* **34,** 583 (1973).
3. D. BEBEL, G. PAUSEWANG, AND W. VIEBAHN, *Z. Naturforsch. B: Anorg. Chem., Org. Chem.* **22,** 1219 (1967); *Z. Anorg. Allg. Chem.* **387,** 161 (1972).
4. P. DARRIET, M. RAT, J. GALY, AND P. HAGENMULLER, *Mater. Res. Bull.* **6,** 1305 (1971).
5. C. MICHAEL AND B. RAVEAU, *Mater. Res. Bull.* **8,** 451 (1973).
6. A. W. SLEIGHT, J. E. GULLEY, AND T. BERZINS, *Adv. Chem. Ser.* **163,** 195–204.
7. C. MICHEL AND B. RAVEAU, *C. R. Seances Acad. Sci., Ser. C* **268,** 323 (1969); M. HERVIEU, C. MICHEL, AND B. RAVEAU, *Bull. Soc. Chim. Fr.* **11,** 3939 (1971).
8. G. ORY, F. FOURQUET, C. JACOBONI, P. MIRANDAY, AND R. DEPAPE, *C. R. Seances Acad. Sci., Ser. C* **273,** 747 (1971).
9. A. W. SLEIGHT, F. C. ZUMSTEG, J. R. BARKLEY, AND J. E. GULLEY, *Mater. Res. Bull.* **13,** 1247 (1978).

10. J. L. Fourquet, C. Jacoboni, and R. DePape, *Acta Crystallogr. Sect. B* **25,** 1570 (1979).

11. J. Grins, M. Nygren, and T. Wallin, *Electrochim. Acta* **24,** 803 (1979); *Mater. Res. Bull.* **15,** 53 (1980).

12. C. Michel, D. Groult, and B. Raveau, *Mater. Res. Bull.* **8,** 201 (1973); *J. Inorg. Nucl. Chem.* **37,** 247, 251, and 1957 (1975).

13. M. A. Butler and R. Biefeld, *Phys. Rev. B* **19,** 5455 (1979); *Solid State Commun.* **29,** 5 (1979).

14. C. Michel, A. Guyomarc'h, A. Deschanvres, and B. Raveau, *Mater. Res. Bull.* **13,** 197 (1978); C. Michel, A. Guyomarc'h, and B. Raveau, *J. Solid State Chem.* **25,** 251 (1978).

15. J. L. Fourquet, J. Jacoboni, and R. dePape, *Mater. Res. Bull.* **8,** 393 (1973).

16. J. E. Greedan, A. H. O'Reilly, and C. V. Stager, *Phys. Rev. B* **35,** 8770 (1987); C. W. Thompson, D. F. R. Mildner, M. Mehregang, J. Sudd, R. Berliner, and W. B. Yelon, *J. Appl. Crystallogr.* **17,** 385 (1984).

17. H. M. Reitveld, *J. Appl. Crystallogr.* **2,** 65 (1969).

18. M. A. Subramanian and A. W. Sleight, *Mater. Res. Bull.* **21,** 727 (1986).

19. B. T. M. Willis, *Acta Crystallogr.* **18,** 75 (1965).

20. B. Dawson, A. C. Hurley, and V. W. Maslen, *Proc. R. Soc. London, Ser. A* **298,** 289 (1967).

21. C. K. Johnson, *Acta Crystallogr. Sect. A* **25,** 187 (1969).

22. J. S. Kasper and K. W. Browall, *J. Solid State Chem.* **13,** 49 (1975).

23. B. T. M. Willis, *Acta. Crystallogr. Sect. A* **25,** 75 (1969).

24. T. Yamanaka, Y. Takeuchi, and M. Tokonami, *Acta. Crystallogr. Sect. B* **40,** 96 (1984).

25. A. K. Jonscher, "Dielectric Relaxation in Solids," Chelsea Dielectric Press, London (1983).